

## Research Article

# MHC I tetramer staining tends to overestimate the number of functionally relevant self-reactive CD8 T cells in the preimmune repertoire

Hanspeter Pircher<sup>1</sup>, Daniel D. Pinschewer<sup>2</sup> and Thomas Boehm<sup>1,3</sup>

<sup>1</sup> Department of Developmental Immunology, Max Planck Institute of Immunobiology and Epigenetics, Freiburg im Breisgau, Germany

<sup>2</sup> Division of Experimental Virology, Department of Biomedicine, University of Basel, Basel, Switzerland

<sup>3</sup> Faculty of Medicine, University of Freiburg, Freiburg im Breisgau, Germany

Previous studies that used peptide-MHC (pMHC) tetramers (tet) to identify self-specific T cells have questioned the effectiveness of thymic-negative selection. Here, we used pMHCI tet to enumerate CD8 T cells specific for the immunodominant gp33 epitope of lymphocytic choriomeningitis virus glycoprotein (GP) in mice transgenically engineered to express high levels of GP as a self-antigen in the thymus. In GP-transgenic mice (GP<sup>+</sup>), monoclonal P14 TCR<sup>+</sup> CD8 T cells that express a GP-specific TCR could not be detected by gp33/D<sup>b</sup>-tet staining, indicative of their complete intrathymic deletion. By contrast, in the same GP<sup>+</sup> mice, substantial numbers of polyclonal CD8 T cells identifiable by gp33/D<sup>b</sup>-tet were present. The gp33-tet staining profiles of polyclonal T cells from GP<sup>+</sup> and GP-negative (GP<sup>-</sup>) mice were overlapping, but mean fluorescence intensities were ~15% lower in cells from GP<sup>+</sup> mice. Remarkably, the gp33-tet<sup>+</sup> T cells in GP<sup>+</sup> mice failed to clonally expand after lymphocytic choriomeningitis virus infection, whereas those of GP<sup>-</sup> mice did so. In Nur77<sup>GFP</sup>-reporter mice, dose-dependent responses to gp33 peptide-induced TCR stimulation revealed that gp33-tet<sup>+</sup> T cells with high ligand sensitivity are lacking in GP<sup>+</sup> mice. Hence, pMHCI tet staining identifies self-specific CD8 T cells but tends to overestimate the number of truly self-reactive cells.

**Keywords:** Clonal deletion · gp33 epitope · MHC-tetramers · Self-reactive T cells



Additional supporting information may be found online in the Supporting Information section at the end of the article.

## Introduction

The development of peptide-MHC (pMHC) multimers to trace antigen-specific T cells by flow cytometry has revolutionized the analysis of T-cell responses [1]. These reagents, mostly used as tetrameric complexes, allow direct visualization, quantification,

and phenotypic characterization of T cells specific for microbial, tumor, and vaccine antigens [2–4]. They have also been exploited to determine T-cell frequencies for antigens in unprimed individuals. In such preimmune repertoires, naïve T-cell frequencies range from 1 to 100 peptide antigen-specific cells per 10<sup>6</sup> T cells. Due to this low frequency, pMHC tetramer (tet) staining in naïve hosts is usually combined with magnetic particle-based cell enrichment [5, 6]. With this technique, termed pMHC tet-based enrichment, T-cell frequencies for a number of epitopes from self and foreign

**Correspondence:** Prof. Hanspeter Pircher  
e-mail: pircher@ie-freiburg.mpg.de

antigens have been determined in human and mouse preimmune repertoires [7, 8].

pMHC tet-based enrichment has also been used to determine mechanisms of CD4 T-cell tolerance induction in polyclonal settings [9–12]. In sum, these data indicated that CD4 T-cell tolerance in polyclonal conditions is established by different mechanisms according to self-peptide expression patterns. In contrast to previous findings with TCR-transgenic (tg) models [13], a complete clonal deletion of polyclonal CD4 T cells to self-antigens was rarely observed. A similar discrepancy between TCR-tg and polyclonal T cells has also been noted for  $\gamma\delta$  T cells specific for a minor histocompatibility gene [14]. Moreover, a study by Yu et al. [15] with human lymphocytes showed that self-specific CD8 T cells identified by pMHC tet staining were present in frequencies similar to those specific for nonself-antigens. This led the authors to conclude that clonal deletion only prunes but does not eliminate self-specific CD8 T cells. This provocative conclusion seems to be at odds with earlier studies claiming that thymic-negative selection is very sensitive to low levels of self-antigen expression [16–19].

To reassess the effectiveness of thymic-negative selection, we analyzed CD8 T cells specific for the gp33 epitope of lymphocytic choriomeningitis virus (LCMV) glycoprotein (GP) in tg mice with robust thymic LCMV GP expression. In essence, our data reveal a striking discrepancy between pMHC tet binding and pMHC tet-induced CD8 T-cell responses. Hence, pMHC tet staining assesses frequencies of self-epitope-binding CD8 T cells but tends to overestimate the number of cells in the preimmune repertoire that can respond to functionally relevant peptide antigen concentrations.

## Results

### Efficient clonal deletion of gp33-tet<sup>+</sup> P14 $\alpha\beta$ T cells in GP<sup>+</sup> mice

In our study, we used tg mice that express the GP of LCMV under the control of different promoters (referred to as GP<sup>+</sup> mice here). Thus, in our tg lines, a viral protein assumes the characteristics of a thymically expressed self-antigen, which affords us the possibility to examine the immune response to this viral-turned-self-antigen by LCMV infection. In MHC1.GP<sup>+</sup> mice, the LCMV GP cDNA is driven by an MHC class I promoter, leading to robust GP expression predominantly in lymphoid organs, including the thymus (Supporting Information Fig. 1A). In CAG.GP<sup>+</sup> mice, the expression of LCMV GP cDNA—linked via an internal ribosomal entry site (IRES) to a yellow fluorescence protein (YFP)-encoding cassette—is driven by the ubiquitous chicken  $\beta$ -actin promoter in the CAG element inserted into the ROSA26 locus [20]. As expected, substantial transgene expression, as visualized by the YFP-reporter, was detected in the thymus of these mice, including CD45<sup>+</sup> hematopoietic cells, dendritic cells, and cortical and medullary thymic epithelial cells (Supporting Information Fig. 1B). Finally, Foxn1.GP<sup>+</sup> mice predominantly express the LCMV-

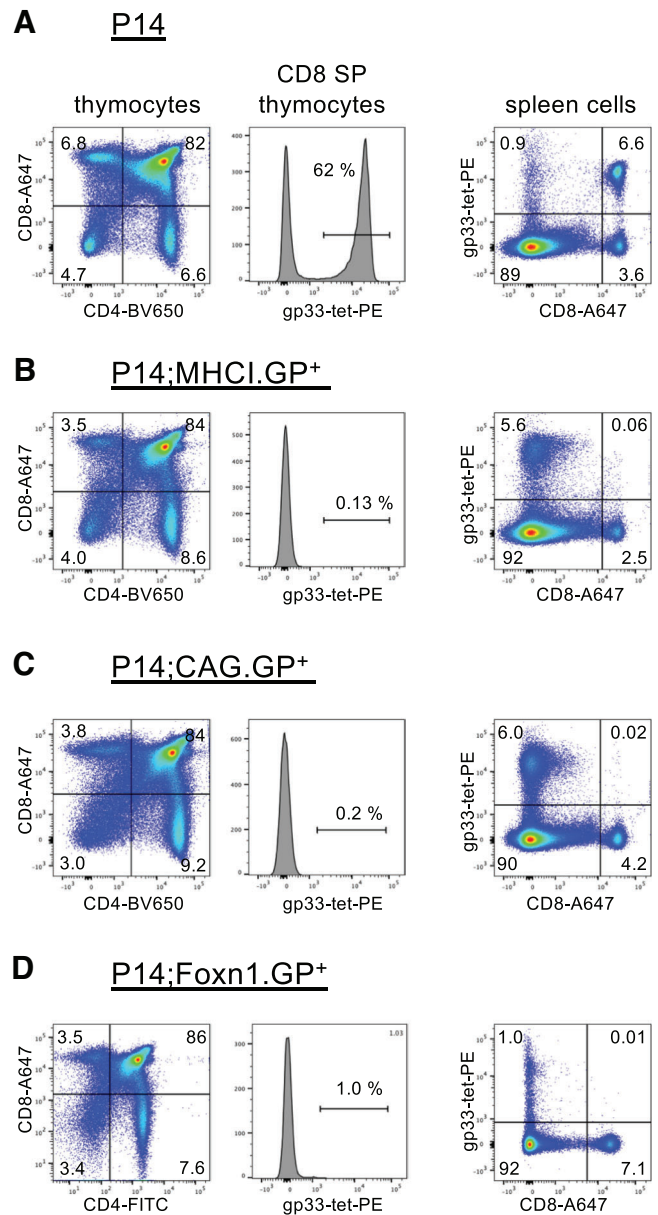


**Figure 1.** Clonal deletion of gp33-tet<sup>+</sup> P14  $\alpha\beta$  T cells in GP<sup>+</sup> mice: (A–D) representative flow cytometry dot plots and histograms gated on total thymocytes (left), CD8 single positive (SP) thymocytes (middle) and spleen cells (right) from mice with the indicated genotypes. Data are representative of the analysis of two-to-three mice per group.

GP–IRES–YFP cassette in cortical and medullary thymic epithelial cells in the thymus (Supporting Information Fig. 1C).

To determine the tolerizing effect of LCMV GP expression on the development of monoclonal GP-specific CD8 T cells, we bred the different GP<sup>+</sup> lines with P14 TCR-tg mice specific for the immunodominant gp33 epitope of LCMV GP presented by H-2D<sup>b</sup>. In the P14 mice used here (line 318), ~60% of CD8 single positive (SP) thymocytes and of peripheral CD8 T cells express the gp33-specific P14 TCR identified by gp33/D<sup>b</sup>-tet (Fig. 1A). In P14;MHC1.GP<sup>+</sup>, P14;CAG.GP<sup>+</sup>, and P14;Foxn1.GP<sup>+</sup> mice, however, gp33-tet<sup>+</sup> cells were hardly detectable in the thymic CD8

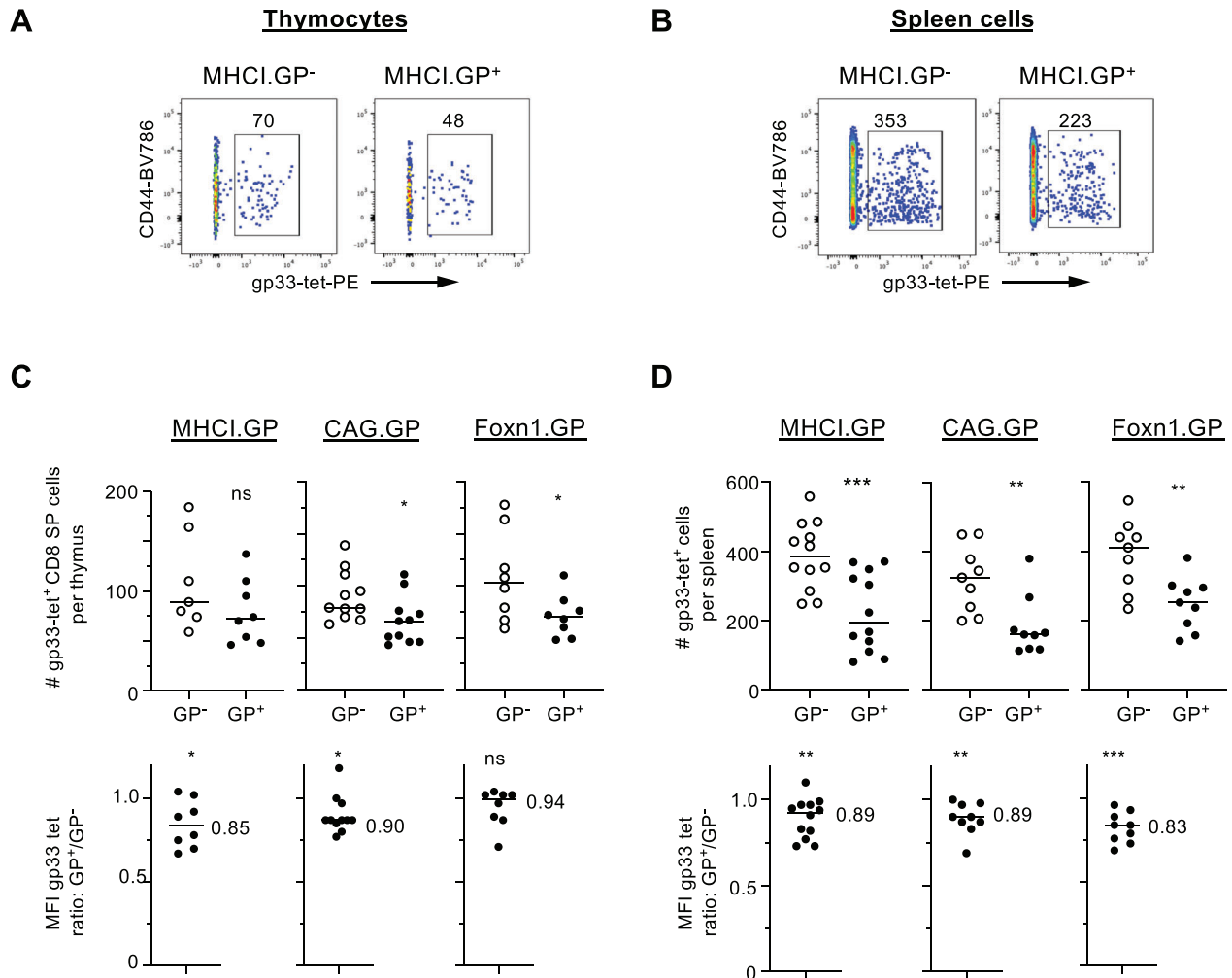


**Figure 2.** Substantial numbers of gp33-tet<sup>+</sup> T cells are present in GP<sup>+</sup> mice: (A and B) representative flow cytometry dot plots gated on CD8 single positive (SP) thymocytes (A) and CD8 spleen cells (B) following gp33/D<sup>p</sup>-tet-based enrichment. The numbers above the gate indicate total numbers of gp33-tet<sup>+</sup> cells recovered from thymus and spleen of one mouse in the sample shown; (C and D) total numbers of gp33-tet<sup>+</sup> CD8 SP thymocytes (C) and gp33-tet<sup>+</sup> CD8 spleen cells (D) isolated from thymi and spleen of mice with the indicated genotypes. The MFI gp33-tet<sup>+</sup> ratios displayed at the bottom were calculated on pairs of gp33-tet<sup>+</sup> cells from GP<sup>+</sup> and GP<sup>-</sup> mice that were analyzed in parallel; average values are indicated. Each data point in the scatter plots represents an individual mouse. Data are pooled from 8 to 12 independent experiments for each group ( $n = 8$ –12 per group). Statistical tests: ns, not significant; \* $p < 0.05$ ; \*\* $p < 0.01$ ; \*\*\* $p < 0.001$ ; unpaired t-test for top graphs; single sample t-test for bottom graphs for the significance between observed means and the hypothetical mean of 1.

SP subsets and in peripheral CD8 T cells (Fig. 1B–D and Supporting Information Fig. 2). In P14;MHCI.GP<sup>+</sup> and P14;CAG.GP<sup>+</sup> mice, enlarged populations of gp33-tet<sup>+</sup> CD8-negative cells were observed; these cells did also not express CD4 (Supporting Information Fig. 3). CD4<sup>-</sup>CD8<sup>-</sup> double negative T cells have been observed previously in CD8 TCR-tg mice with ubiquitous self-antigen expression [21]. These cells are thought to escape negative selection because MHC I-restricted antigen recognition usually requires CD8 co-expression [22, 23]. The cells do not require positive selection by thymic MHC molecules but are selected by nominal antigens on hemopoietic cells [24]. Moreover, they display properties of  $\gamma/\delta$ -lineage cells and arise due to premature expression of the tg  $\alpha\beta$  TCR chains in early double negative thymocytes [25–28]. In sum, our data show that thymic

GP expression in the three GP<sup>+</sup> lines studied here resulted in a near complete clonal deletion of gp33-tet<sup>+</sup> P14 CD8 T cells in the thymus.

### Polyclonal gp33-tet<sup>+</sup> T cells are present in GP<sup>+</sup> mice in substantial numbers

Next, polyclonal gp33-tet<sup>+</sup> CD8 T cells in the thymi and spleen of MHCI.GP<sup>+</sup>, CAG.GP<sup>+</sup>, and Foxn1.GP<sup>+</sup> mice were enumerated by pMHC tet-based enrichment. In striking contrast to gp33-tet<sup>+</sup> P14 T cells, substantial numbers of polyclonal gp33-tet<sup>+</sup> CD8 SP thymocytes were present in all GP<sup>+</sup> mice (Fig. 2A,C). In comparison to GP-negative litter mates, their numbers were reduced by

26–34%, and mean fluorescence intensities (MFIs) of gp33-tet staining were decreased by 6–15%. The specificity of the gp33-tet staining was tested by examining CD4 SP thymocyte subsets after enrichment; in all samples, only a very few gp33-tet<sup>+</sup> cells were detected in these cell subsets (Supporting Information Fig. 4). To determine whether GP expression in the thymus leads to increased TCR signaling in gp33-tet<sup>+</sup> CD8 SP thymocytes, we used Nur77<sup>GFP</sup>-reporter mice [29]. The results show that Nur77<sup>GFP</sup> expression levels in gp33-tet<sup>+</sup> CD8 SP thymocytes were comparable in Nur77<sup>GFP</sup>;MHCI.GP<sup>+</sup> and Nur77<sup>GFP</sup>;MHCI.GP<sup>-</sup> mice (Supporting Information Fig. 5).

The analysis of peripheral polyclonal CD8 T cells confirmed the presence of gp33-tet<sup>+</sup> T cells in GP<sup>+</sup> mice (Fig. 2B,D). On average, ~200 gp33-tet<sup>+</sup> CD8 T cells per spleen were recovered from GP<sup>+</sup> mice, in comparison to ~400 cells from GP-negative littermate control mice. The specificity of the gp33-tet staining was controlled with spleen cells from OT-I TCR-tg mice, which lack a polyclonal repertoire [30]. Here, only very few (<5) gp33-tet<sup>+</sup> T cells per spleen were detected (Supporting Information Fig. 6A). The gp33-tet staining profiles in T cells from GP<sup>+</sup> and GP<sup>-</sup> mice overlapped, but MFIs in GP<sup>+</sup> mice were slightly lower than those of GP<sup>-</sup> mice, resulting in GP<sup>+</sup>/GP<sup>-</sup> gp33-tet MFI ratios of 0.83–0.89 on average (Fig. 2D, bottom and Supporting Information Fig. 6B). Of note, the decreased gp33-tet staining intensity in T cells from GP<sup>+</sup> mice was not due to lower TCR expression levels (Supporting Information Fig. 6C). With respect to cell surface markers, gp33-tet<sup>+</sup> T cells from both GP<sup>+</sup> and GP<sup>-</sup> mice lacked signs of activation; they predominantly showed a naïve CD44<sup>low</sup>CD62L<sup>high</sup> phenotype, did not express activation markers (CD69 and PD-1), and also displayed comparable levels of CD5 (Supporting Information Fig. 7). In sum, considerable numbers of naïve phenotype gp33-tet<sup>+</sup> CD8 T cells are present in mice with robust thymic GP expression.

### gp33-tet<sup>+</sup> T cells with the fixed P14 TCR-β chain are efficiently deleted in GP<sup>+</sup> mice

The different degrees in clonal deletion of P14 αβ versus polyclonal T cells led us to analyze mice that express the P14 TCR-β chain on almost all CD4 and CD8 T cells. These P14 TCR-β-tg mice (P14β) exhibit tight allelic exclusion for endogenous TCR-β chains and display a polyclonal TCR-α chain repertoire [31, 32]. In P14β mice without GP expression, the numbers of gp33-tet<sup>+</sup> CD8 T cells were comparable to WT mice (Fig. 3A, first and second rows). In GP expressing P14β;MHCI.GP<sup>+</sup> and P14β;CAG.GP<sup>+</sup> mice, however, gp33-tet<sup>+</sup> T cells were almost absent (Fig. 3A, third and fourth rows). The pMHC tet staining intensities of gp33-tet<sup>+</sup> CD8 T cells in P14β mice without GP expression were increased ~3-fold when compared to WT mice and reached levels almost comparable to P14 αβ T cells (Fig. 3B). The few remaining gp33-tet<sup>+</sup> cells in P14β;MHCI.GP<sup>+</sup> and P14β;CAG.GP<sup>+</sup> mice, however, showed strongly decreased tet staining intensities resulting in low gp33-tet MFI ratios (GP<sup>+</sup>/GP<sup>-</sup>) of ~0.18 on average (Fig. 3C). As pMHC tet staining intensity is thought to correlate with TCR avid-

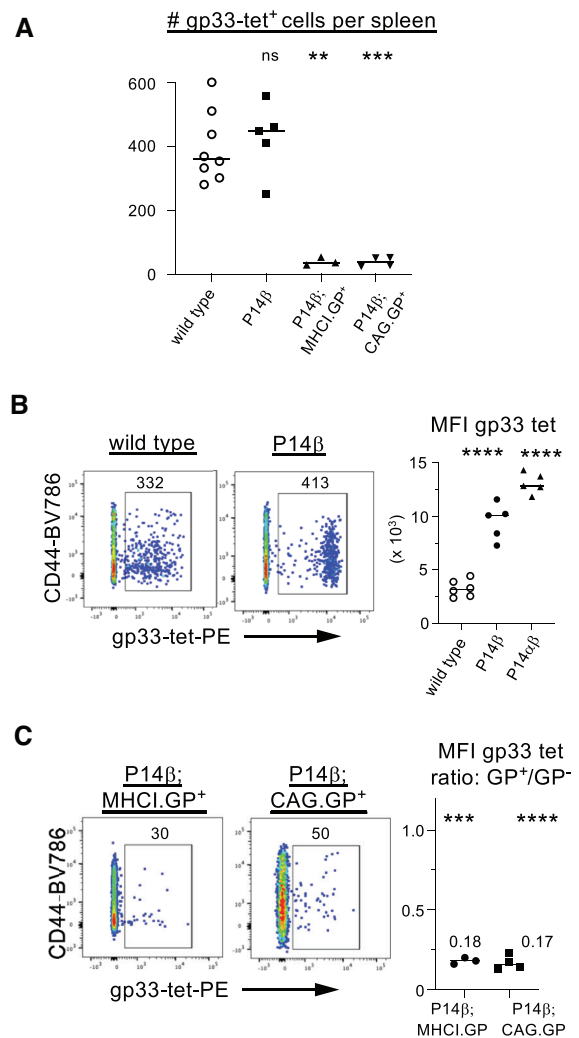


**Figure 3.** gp33-tet<sup>+</sup> T cells with P14 βTCR are deleted in GP<sup>+</sup> mice: (A) total numbers of gp33-tet<sup>+</sup> T cells recovered from spleen of mice with the indicated genotypes after enrichment; (B) left: representative flow cytometry dot plots gated on CD8 T cells following gp33/D<sup>b</sup>-tet-based enrichment of spleen cells from C57BL/6 WT and P14 TCR-β-tg mice analyzed in parallel; right: MFIs of gp33-tet staining of spleen cells from mice with the indicated genotypes; (C) left: representative flow cytometry dot plots gated on CD8 T cells following gp33/D<sup>b</sup>-tet-based enrichment of spleen cells from mice with the indicated genotypes. The numbers above the gate in the dot plots indicate total numbers of gp33-tet<sup>+</sup> T cells recovered from the spleen of one mouse in the sample shown; right: MFI gp33-tet<sup>+</sup> ratios calculated on pairs of gp33-tet<sup>+</sup> CD8 spleen cells from the indicated P14β.GP<sup>+</sup> and P14β.GP<sup>-</sup> mice that were analyzed in parallel. Each data point in the scatter plots represents an individual mouse. Data are pooled from three to five independent experiments for each group (n = 3–5 per group). Statistical tests: \*\*p < 0.01; \*\*\*p < 0.001; \*\*\*\*p < 0.0001; unpaired t-test for parts (A) and (B), single sample t-test for part (C) for the significance between observed means and the hypothetical mean of 1.

ity [33–37], these data indicate that the P14 TCR-β chain selects for TCRs that bind the gp33 epitope with high avidity. In addition, the data demonstrate that P14β T cells expressing high avidity gp33-specific antigen receptors are efficiently deleted in GP<sup>+</sup> mice.

## Polyclonal gp33-tet<sup>+</sup> T cells in GP<sup>+</sup> mice fail to clonally expand after LCMV infection

Given that substantial numbers of polyclonal gp33-tet<sup>+</sup> T cells are present in GP<sup>+</sup> mice, it was important to test their functional activity. To this end, we examined the response of GP<sup>+</sup> and GP<sup>-</sup> mice to the acute provision of GP via LCMV infection and determined the numbers of gp33-tet<sup>+</sup> T cells without enrichment at day 8 postinfection. Infection of MHCI.GP<sup>-</sup> control mice with the Armstrong strain of LCMV led to a vigorous expansion of both gp33-tet<sup>+</sup> and np396-tet<sup>+</sup> CD8 T cells. In striking contrast, only a very few gp33-tet<sup>low</sup> CD8 T cells were detectable in LCMV-infected MHCI.GP<sup>+</sup> mice, although an increase of np396-tet<sup>+</sup> T cells was recorded similar to infected GP<sup>-</sup> mice (Fig. 4A and Supporting Information Fig. 8). These results indicate that the observed nonresponsiveness of gp33-tet<sup>+</sup> T cells in MHCI.GP<sup>+</sup> mice is antigen-specific and not the result of a generally impaired immune reactivity. Of note, LCMV-infected MHCI.GP<sup>+</sup> mice did not show disease symptoms or increased weight loss compared to MHCI.GP<sup>-</sup> mice (Supporting Information Fig. 9).

To exclude the possibility that the failure to induce a gp33-specific T-cell response in LCMV-infected GP<sup>+</sup> mice despite the presence of gp33-tet<sup>+</sup> T cells is a peculiarity of the gp33 epitope, we proceeded to analyze the effect of a second antigen. To this end, we analyzed tg mice expressing the LCMV nucleoprotein (NP) under the control of the H-2K<sup>b</sup> MHCI promotor (referred to as NP<sup>+</sup> mice here, [38]). This allowed us to directly evaluate the presumed reciprocal outcome of an LCMV infection. NP-specific CD8 T cells in the polyclonal repertoire were enumerated with np396/D<sup>b</sup> tet that contained the immunodominant CD8 T-cell epitope of LCMV NP. Similar to the situation in GP<sup>+</sup> mice, np396/D<sup>b</sup> tet<sup>+</sup> CD8 T cells were present in the naïve repertoire of NP<sup>+</sup> mice. Compared to NP<sup>-</sup> mice, the numbers of np396/D<sup>b</sup> tet<sup>+</sup> CD8 T cells were reduced about twofold, and MFIs of tet staining were 26% lower, on average (Fig. 4B). Importantly, and in analogy to GP<sup>+</sup> mice, an LCMV infection of NP<sup>+</sup> mice also failed to induce clonal expansion of np396-tet<sup>+</sup>, but not of gp33-tet<sup>+</sup> CD8 T cells (Fig. 4C). Thus, our results with self-antigens of viral origin indicate that CD8 T cells detectable by self-antigen-specific tet appear to be generally nonresponsive to stimulation by their cognate antigen in the context of a viral infection. Similar to the outcome in MHCI.GP<sup>+</sup> mice, gp33-tet<sup>+</sup> T cells in CAG.GP<sup>+</sup> and in Foxn1.GP<sup>+</sup> mice also failed to clonally expand after the LCMV Armstrong infection (Fig. 4D,E).

Adoptive cell transfers were performed to determine whether the gp33-specific nonresponsiveness in GP<sup>+</sup> mice was T cell-intrinsic. For these experiments, we used total T cells from Foxn1.GP<sup>+</sup> mice as donor cells because these cells lack GP expression in contrast to T cells from MHCI.GP<sup>+</sup> and CAG.GP<sup>+</sup> mice. Total splenic T cells from Foxn1.GP<sup>+</sup> and Foxn1.GP<sup>-</sup> mice (both exhibiting the Thy1.2 allotype marker) were adoptively transferred into B6.Thy1.1<sup>+</sup> recipients, followed by LCMV Armstrong infection. At day 8 postinfection, the gp33-specific CD8 T-cell response was determined in donor and host compartments. In recipients that received T cells from Foxn1.GP<sup>-</sup> mice, a gp33-

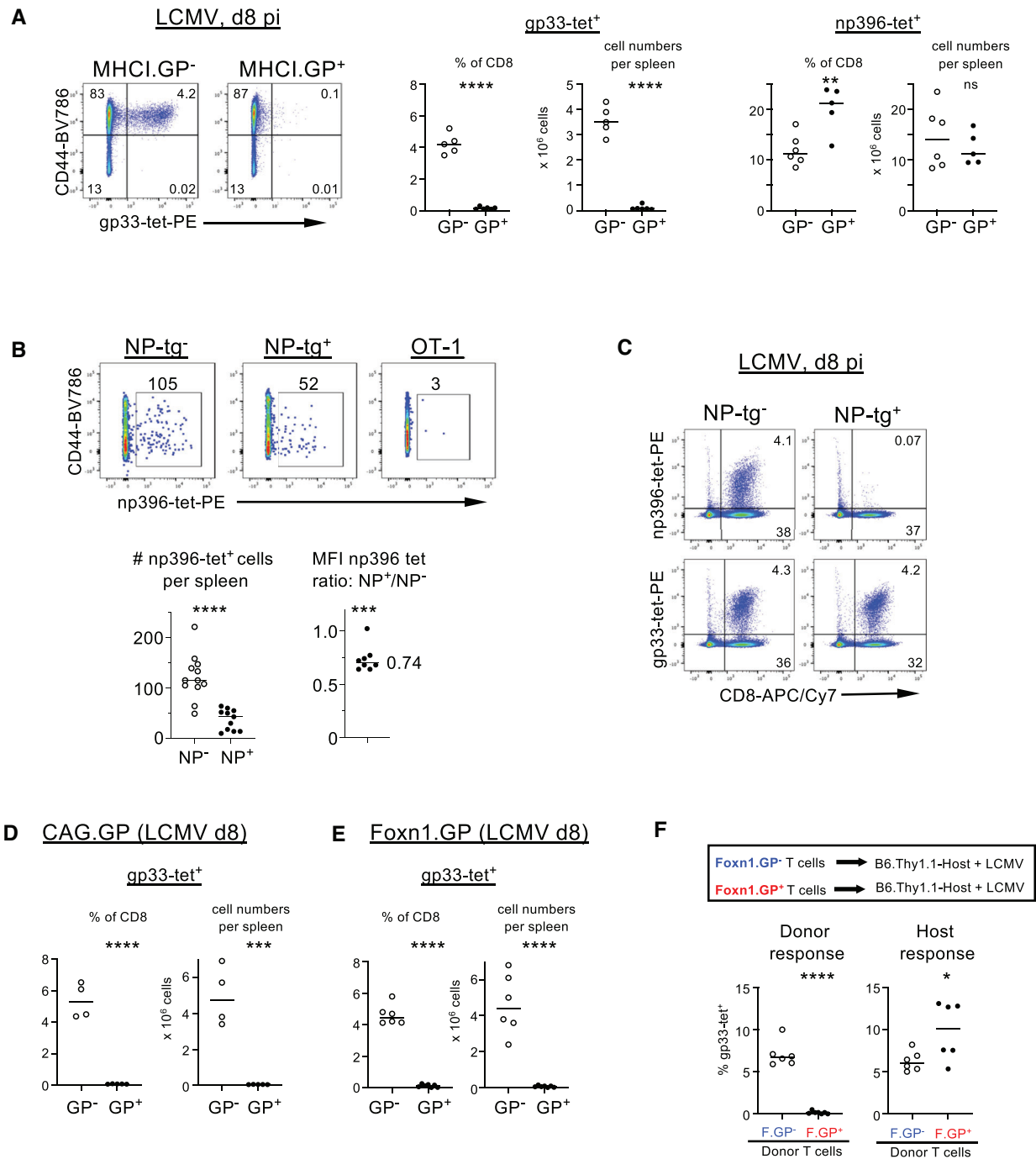
specific response was observed in both donor and host T cells. In contrast, in recipients of T cells from Foxn1.GP<sup>+</sup> mice, only host but not donor T cells mounted a gp33-specific response (Fig. 4F). If co-transferred regulatory T cells would cause the gp33-specific nonresponsiveness, the gp33-specific response of host T cells should also be affected. Thus, these data indicate that the gp33-specific nonresponsiveness in Foxn1.GP<sup>+</sup> mice is T cell-intrinsic.

## gp33-tet<sup>+</sup> T cells with high ligand sensitivity are missing in GP<sup>+</sup> mice

Next, we assessed TCR signaling in gp33-tet<sup>+</sup> T cells using Nur77<sup>GFP</sup>-reporter mice [29]. First, we compared Nur77<sup>GFP</sup> expression in steady state of unstimulated Nur77<sup>GFP</sup>;MHCI.GP<sup>+</sup> and Nur77<sup>GFP</sup>;MHCI.GP<sup>-</sup> mice. In both types of mice, a similar small portion (~10%) of gp33-tet<sup>+</sup> T cells expressed Nur77<sup>GFP</sup> at low-intensity levels (Fig. 5A, first row and Fig. 5B). This indicated that the TCRs of gp33-tet<sup>+</sup> T cells in MHCI.GP<sup>+</sup> mice were not specifically triggered by self-GP expression. Second, we examined whether Nur77<sup>GFP</sup> expression in gp33-tet<sup>+</sup> T cells could be induced by exposure to GP-expressing spleen cells. Indeed, the adoptive transfer of MHCI.GP<sup>+</sup> splenocytes induced Nur77<sup>GFP</sup> expression in MHCI.GP<sup>-</sup> but not in MHCI.GP<sup>+</sup> mice (Fig. 5A, second row and Fig. 5B). These data show that the TCRs of gp33-tet<sup>+</sup> cells in MHCI.GP<sup>+</sup> mice are not triggered by their nominal self-antigen indicating that the binding of nominal pMHCI tet does not necessarily correlate with pMHCI-specific T-cell responsiveness.

To examine whether TCR signaling in gp33-tet<sup>+</sup> T cells from MHCI.GP<sup>+</sup> mice could be induced by high doses of antigen, mice were injected with different amounts of synthetic gp33 peptide; Nur77<sup>GFP</sup> expression was determined 6 h later. Interestingly, injection of a high dose of gp33 peptide (500 µg per mouse) induced robust Nur77<sup>GFP</sup> expression (~40–60%) in gp33-tet<sup>+</sup> T cells not only from MHCI.GP<sup>-</sup> but also from MHCI.GP<sup>+</sup> mice (Fig. 5A, third row). At this high antigen dose, Nur77<sup>GFP</sup> expression levels were similar in both types of mice but the percent values of Nur77<sup>GFP</sup> cells were somewhat decreased in MHCI.GP<sup>+</sup> mice (Fig. 5C,D, left panels). Induction of Nur77<sup>GFP</sup> was antigen-specific, because CD8 T cells with other antigen specificities did not upregulate Nur77<sup>GFP</sup> after gp33 peptide injection (Supporting Information Fig. 10). At decreasing gp33 peptide doses (100 and 20 µg per mouse), the percent values of Nur77<sup>GFP</sup> cells within the gp33-tet<sup>+</sup> T-cell subsets decreased in both groups (Fig. 5A, fourth and fifth rows, and Fig. 5C). However, Nur77<sup>GFP</sup> intensity levels in gp33-tet<sup>+</sup> T cells from MHCI.GP<sup>-</sup> mice remained at a high level in contrast to cells from MHCI.GP<sup>+</sup> mice that showed decreased Nur77<sup>GFP</sup> intensity at lower antigen doses (Fig. 5D, middle and right panels).

Moreover, gp33-tet<sup>high</sup> T cells expressing Nur77<sup>GFP</sup> at high levels (indicated by small black arrows in Fig. 5A, fourth and fifth rows) were substantially more numerous in MHCI.GP<sup>-</sup> compared to MHCI.GP<sup>+</sup> mice. To quantify this observation, we determined the relative gp33-tet MFIs in the responding Nur77<sup>GFP</sup> cell populations. As shown in Fig. 5E, these values were significantly



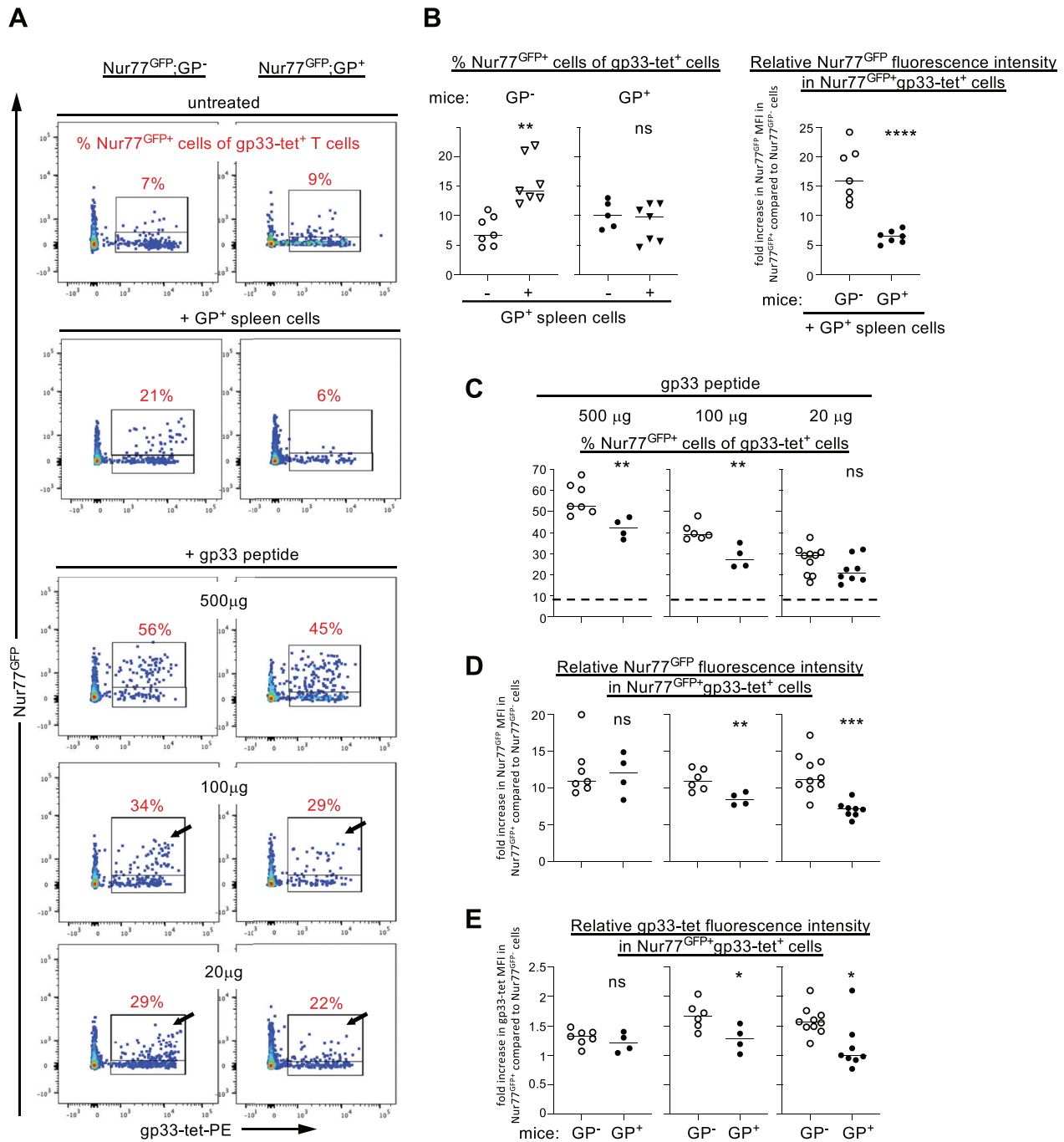


**Figure 5.** gp33-specific TCR signaling in Nur77<sup>GFP</sup>-reporter mice: (A) representative flow cytometry dot plots gated on CD8 T cells following gp33/D<sup>b</sup>-tet-based enrichment of spleen cells from Nur77<sup>GFP</sup>;MHCII.GP<sup>-</sup> (panels in left column) and Nur77<sup>GFP</sup>;MHCII.GP<sup>+</sup> mice (panels in right column). Plots are shown for untreated mice (first row), for mice after stimulation with MHCII.GP<sup>+</sup> splenocytes (second row), and for mice after injection of different amounts of gp33 peptide (rows 3–5). The numbers in red in the plots indicate percentages of Nur77<sup>GFP</sup>+ cells among gp33-tet<sup>+</sup> T cells located in the upper gates. The small black arrows in the fourth and fifth row points to gp33-tet<sup>high</sup> T cells expressing Nur77<sup>GFP</sup> at high levels; (B–E) combined analysis of the experiments illustrated in part (A); (B) left panel: percentages of Nur77<sup>GFP</sup>+ cells in the gp33-tet<sup>+</sup> T-cell populations of GP<sup>-</sup> and GP<sup>+</sup> mice with and without injection of MHCII.GP<sup>+</sup> splenocytes; right panel: relative Nur77<sup>GFP</sup> fluorescence intensities in Nur77<sup>GFP</sup>+gp33-tet<sup>+</sup> cells of GP<sup>-</sup> and GP<sup>+</sup> mice after injection of MHCII.GP<sup>+</sup> spleen cells. The fold increase in Nur77<sup>GFP</sup> fluorescence was calculated by comparison to MFI values in Nur77<sup>GFP</sup>- cells situated in the lower gates depicted in part (A); (C) percentages Nur77<sup>GFP</sup>+ cells of gp33-tet<sup>+</sup> T cells in GP<sup>-</sup> mice (left columns) and GP<sup>+</sup> mice (right columns) after injection of different amounts of gp33 peptide. The dashed lines represent the percentage of Nur77<sup>GFP</sup>+ cells of gp33-tet<sup>+</sup> T cells in untreated mice; (D) increase in Nur77<sup>GFP</sup> fluorescence intensities in Nur77<sup>GFP</sup>+gp33-tet<sup>+</sup> cells in GP<sup>-</sup> (left columns) and GP<sup>+</sup> mice (right columns) after gp33 peptide injection, calculated as described in part (B); (E) relative gp33-tet fluorescence intensities in Nur77<sup>GFP</sup>+gp33-tet<sup>+</sup> cells in GP<sup>-</sup> (left columns) and GP<sup>+</sup> mice (right columns) after gp33 peptide injection, calculated as described in part (B). Each data point in the scatter plots represents an individual mouse. Data are pooled from four to ten independent experiments for each group (*n* = 4–10 per group). Statistical tests: ns, not significant; \**p* < 0.05; \*\**p* < 0.01; \*\*\**p* < 0.001; \*\*\*\**p* < 0.0001 unpaired t-test.

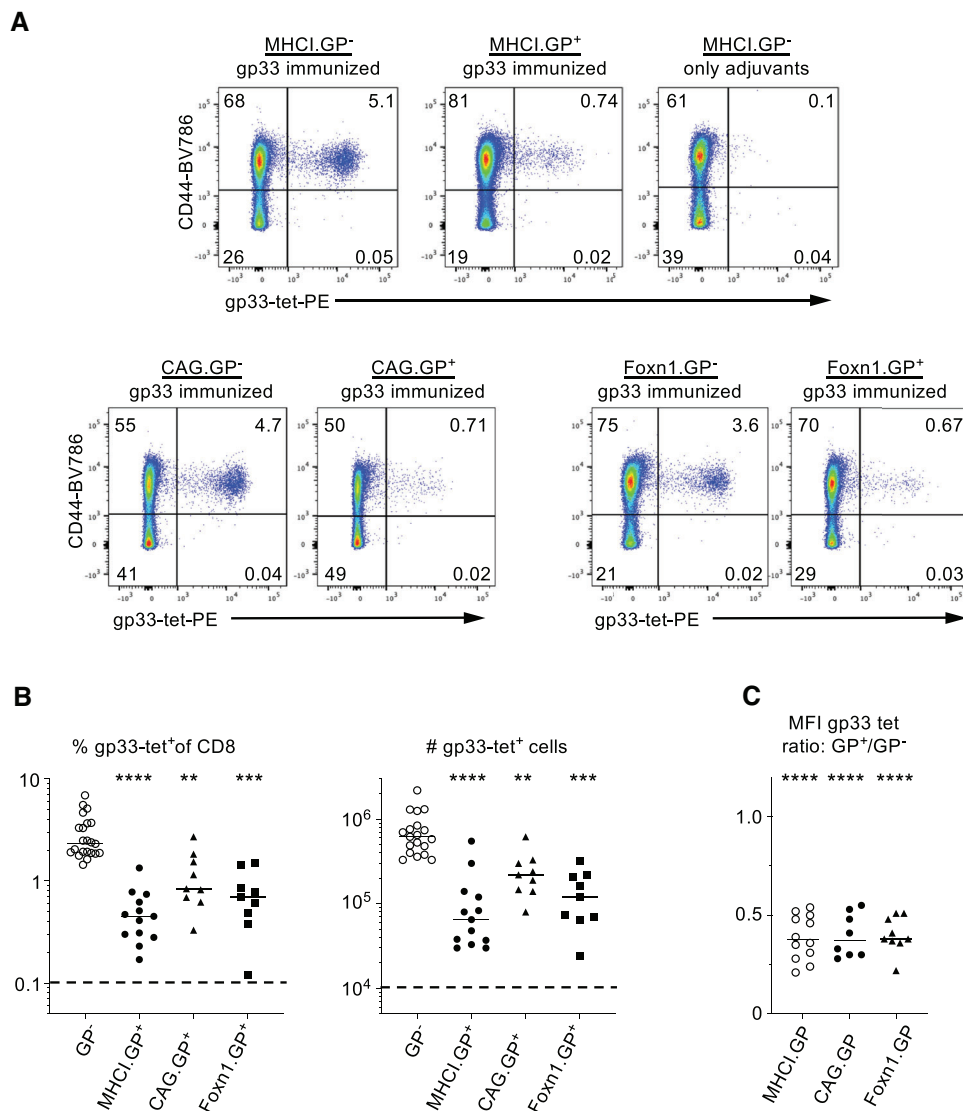


**Figure 6.** Outcome of gp33 peptide immunization in GP<sup>+</sup> and GP<sup>-</sup> mice: (A) representative flow cytometry dot plots gated on splenic CD8 T cells isolated from mice with the indicated genotypes 8 days after gp33 peptide (500  $\mu$ g) immunization. Cells were stained without previous tet-based enrichment. CD8 T cells from MHCI.GP<sup>-</sup> mice that received only anti-CD40 mAb and poly (I:C) were included as a negative control (top row, most right plot); (B) percentages gp33-tet<sup>+</sup> T cells of splenic CD8 T cells (left panel) and total numbers of splenic gp33-tet<sup>+</sup> T cells (right panel) in gp33 peptide-immunized mice of the indicated genotypes. The dashed line represents the detection limit of gp33-tet<sup>+</sup> T cells in spleen without gp33/D<sup>p</sup>-tet-based enrichment; (C) MFI gp33-tet<sup>+</sup> ratios calculated on pairs of gp33-tet<sup>+</sup> CD8 spleen cells from the indicated GP<sup>+</sup> and GP<sup>-</sup> mice that were analyzed in parallel. Each data point in the scatter plots represents an individual mouse. Data are pooled from 12 independent experiments for each group ( $n = 8-21$  per group). Statistical tests: \*\* $p < 0.01$ ; \*\*\* $p < 0.001$ ; \*\*\*\* $p < 0.0001$  unpaired t-test; single sample t-test for part (C) for the significance between observed means and the hypothetical mean of 1.

increased in MHCI.GP<sup>-</sup> compared to MHCI.GP<sup>+</sup> mice at lower peptide antigen doses. Taken together, these data demonstrate that gp33-tet<sup>high</sup> T cells that are capable of inducing substantial Nur77<sup>GFP</sup> levels after triggering with lower doses of gp33 antigen are missing in GP<sup>+</sup> mice.

### gp33 peptide immunization of GP<sup>+</sup> mice predominantly induce expansion of gp33-tet<sup>low</sup> T cells

Finally, we examined whether a proliferative response of gp33-tet<sup>+</sup> T cells could be induced in GP<sup>+</sup> mice by gp33 peptide immu-

nization combined with poly (I:C) and anti-CD40 stimulation as strong adjuvants. This peptide immunization protocol has been shown to induce a potent antigen-specific CD8 T-cell response in mice [39]. Unlike the outcome of LCMV infection (Fig. 4), the immunization of MHCI.GP<sup>+</sup>, CAG.GP<sup>+</sup>, and Foxn1.GP<sup>+</sup> mice with a high dose of gp33 peptide (500  $\mu$ g per mouse) plus adjuvants gave rise to a readily detectable population of gp33-tet<sup>+</sup> CD44<sup>high</sup> T cells at day 8 after priming (Fig. 6A). Nonetheless, frequencies and numbers of the induced gp33-tet<sup>+</sup> T cells were about three- to sixfold lower than in immunized GP<sup>-</sup> control mice (Fig. 6B). At lower peptide doses, the numbers of the induced gp33-tet<sup>+</sup>

T cells in GP<sup>+</sup> mice were near the detection limit of the assay (Supporting Information Fig. 11). More interestingly, the gp33-tet staining intensities of the induced T cells in GP<sup>+</sup> mice were considerably lower than those in GP<sup>-</sup> mice, resulting in tet MFI ratios (GP<sup>+</sup>/GP<sup>-</sup>) of ~0.4 (Fig. 6C). These values are remarkably lower than the corresponding values in the preimmune repertoire (~0.9, Fig. 2D, bottom). Thus, the differences in gp33-tet staining intensities between GP<sup>+</sup> and GP<sup>-</sup> mice were amplified by the gp33 peptide immunization. Of note, the lower gp33-tet staining intensities of the induced T cells in GP<sup>+</sup> mice were not due to decreased TCR expression levels (Supporting Information Fig. 12). The finding that immunogenic gp33 peptide immunization predominantly induced the expansion of gp33-tet<sup>low</sup> T cells in GP<sup>+</sup> mice suggests that the nonresponsiveness of gp33-tet<sup>high</sup> T cells in GP<sup>+</sup> mice is more pronounced than that of gp33-tet<sup>low</sup> T cells.

## Discussion

In mice expressing the GP of LCMV in the thymus, polyclonal GP-specific CD8 T cells identified by gp33-tet are present in substantial numbers. At first glance, it would therefore seem that clonal deletion fails to eliminate self-specific CD8 T cells. However, the additional functional experiments performed here led to a substantially different conclusion. In essence, our data show that despite a seemingly continuous profile of tet staining intensities of polyclonal CD8 T cells, functional assays distinguish two classes of self-antigen-specific tet<sup>+</sup> T cells. T cells expressing TCRs with high ligand sensitivity are efficiently tolerized in GP<sup>+</sup> mice, most likely by clonal deletion, as exemplified by high avidity P14  $\alpha\beta$  and P14 $\beta$  T cells. All cells expressing TCRs that confer little ligand sensitivity for self-antigen remain in the polyclonal repertoire. Importantly, these TCRs are still able to specifically bind cognate pMHC I tet at levels almost comparable to TCRs from WT mice. Their naïve phenotype and the lack of TCR triggering in steady state further indicate that exposure to GP expression is functionally irrelevant for this subset of gp33-tet<sup>+</sup> T cells. Accordingly, these cells fail to clonally expand after LCMV infection; however, the fact that they can be induced to respond when they are exposed to large amounts of antigen may reflect their low avidity TCRs.

There is a number of studies that are relevant to our findings. Yu et al. [15] determined frequencies of human CD8 T cells specific for self and foreign peptide antigens by pMHC I tet staining and found that they were surprisingly similar. Furthermore, they observed that self-specific CD8 T cells failed to proliferate after stimulation with the cognate peptide antigens. This led the authors to conclude that tolerance of self-specific CD8 T cells is predominantly mediated by nondeletional mechanisms, such as induction of T-cell anergy. In our model, gp33-tet<sup>+</sup> T cells in GP<sup>+</sup> mice failed to proliferate after LCMV infection. We rationalize the gp33-specific nonresponsiveness after LCMV infection as resulting from insufficient ligand sensitivity. After immunogenic gp33 peptide immunization, however, we found that the nonresponsiveness of gp33-tet<sup>high</sup> T cells in GP<sup>+</sup> mice was more pronounced than that of gp33-tet<sup>low</sup> T cells. Therefore, T-cell anergy or T-cell

tuning [40] may also play a role in gp33-specific T-cell tolerance induction in GP<sup>+</sup> mice.

Our study shows interesting parallels to a recent report by Truckenbrod et al. [41] who analyzed polyclonal CD8 T cells specific for the melanocyte antigen tyrosinase-related protein 2 (Trp2) in mice expressing or lacking Trp2. Similar to our data, Trp2-tet<sup>+</sup> T cells in *Trp2*<sup>+</sup> mice showed a naïve phenotype. Compared to *Trp2*-deficient mice, their numbers were reduced about twofold, and MFIs of Trp2-tet<sup>+</sup> staining levels were decreased by ~20% in mice expressing Trp2. Trp2-tet<sup>+</sup> T cells were also impaired in clonal expansion and mediated vitiligo less efficiently than cells from Trp2-deficient mice. Nonetheless, there are also important differences to our study. In distinction to the robust thymic self-antigen expression in our model, the level of Trp2 expression in thymic mTECs is probably much lower. One report [42] even suggested that mTECs lack Trp2 expression. Thus, it is unclear whether T-cell tolerance to Trp2 occurs during thymic development or in the periphery. Another difference concerns the outcome of peptide antigen vaccination of tet staining intensities of the responding T cells. In GP<sup>+</sup> mice, immunogenic gp33 peptide immunization induced the expansion of gp33-tet<sup>+</sup> T cells with strongly decreased gp33-tet staining intensities. Unlike these findings, the differences in Trp2-tet<sup>+</sup> staining intensities in the Trp2 model were not amplified by Trp2 peptide antigen immunization.

In mice with a fixed TCR- $\beta$  chain, self-reactive CD8 T cells to HY or OVA could be identified by pMHC I tet staining [33, 37]. Importantly, pMHC I tet staining intensities of these self-reactive T cells were substantially decreased in mice that expressed the model self-antigen; as a result, tet MFI ratios (self<sup>+</sup>/self<sup>-</sup>) of ~0.35 were observed. The selective elimination of T cells expressing high avidity receptors for self-antigens was therefore more noticeable than in our polyclonal GP<sup>+</sup> mice without fixed TCR- $\beta$  chain. Here, the differences in tet staining intensities were subtler (gp33-tet MFI ratio GP<sup>+</sup>/GP<sup>-</sup> ~0.9). In P14 $\beta$ ;GP<sup>+</sup> mice, however, the deletion of gp33-tet<sup>+</sup> T cells expressing high avidity receptors was also much more obvious, and severely decreased gp33-tet<sup>+</sup> MFI ratios (GP<sup>+</sup>/GP<sup>-</sup> ~0.18) were observed. Taken together, these data illustrate that a TCR repertoire built around a fixed TCR- $\beta$  chain favors the generation of higher affinity TCRs; the deletion of such high-affinity TCRs in these models manifests itself more drastically in reduced tet MFI ratios.

Self-specific human CD8 T cells as defined by pMHC I tet binding are frequently detected in healthy unprimed individuals [43–46]. Similar to gp33-tet<sup>+</sup> T cells in GP<sup>+</sup> mice, many of these self-specific T cells may, however, ignore their self-antigens, as they often lack signs of activation and present with naïve phenotypes. Ignorance of T cells to self-antigens is either due to the expression of TCRs with low ligand sensitivity as exemplified here, restricted self-antigen expression in immune-privileged sites, and/or low self-antigen expression levels. T-cell ignorance, however, can be broken by strong antigenic stimulation in mice [47, 48].

Remarkably, although the LCMV infection represents a very potent trigger for CD8 T-cell responses in mice [49], a detectable gp33-tet<sup>+</sup> CD8 T-cell response in GP<sup>+</sup> mice could not be induced

by this means; it could only be induced by high-dose gp33 peptide immunization. How can this finding be rationalized? High-dose gp33 peptide immunization most likely leads to higher levels of gp33/D<sup>b</sup> complexes on the surface of antigen-presenting cells than an LCMV infection. The shift of pMHC occupancy after gp33 peptide priming would then induce a response of even low avidity gp33-tet<sup>+</sup> T cells in GP<sup>+</sup> mice. Although paradoxical at first glance, the very differential reactivity of T cells to gp33 peptide immunization versus LCMV infection strongly supports the notion that responsive gp33-tet<sup>+</sup> T cells in GP<sup>+</sup> mice express low avidity TCRs.

Our conclusion that pMHCI tet staining overestimates the number of antigen-reactive CD8 T cells contrasts with previous findings that pMHCI tet staining underestimates frequencies of antigen-specific CD4 T cells [50]. In particular, low-affinity CD4 T cells unable to bind pMHCI tet were proposed to be the major responders in primary immune responses [51]. On the one hand, this discrepancy can be explained by the different roles that CD4 and CD8 coreceptors play in binding pMHCI- and pMHCI tet, respectively: In contrast to the enhancing effect of CD8 for pMHCI tet binding, CD4 has little influence on TCR/pMHCI-tet interactions [35, 52]. On the other hand, the pMHCI-tet binding studies cited above were performed after antigen challenge, whereas we have determined the number of pMHCI-tet<sup>+</sup> cells in preimmune repertoires. In this context, it is worth noting that mice with a ubiquitous expression of the 2W model antigen also contain a few conventional 2W/I-A<sup>b</sup>-tet<sup>+</sup> CD4 T cells in their preimmune repertoire; these cells exhibit lower tet MFI values than those in WT mice, lack signs of previous activation and do not express an anergic phenotype [12, 53].

Incomplete recruitment of pMHC-tet<sup>+</sup> CD4 and CD8 T cells from the naïve into the immune repertoire has been observed previously in TCR- $\beta$ -chain tg mice [54, 55]. In addition, discrepancy between pMHCI tet binding and reactivity has also been noted in T-cell cultures. For example, Kalergis et al. [56] generated CD8 T-cell hybridomas with mutated TCRs that efficiently bind pMHCI tet but fail to react with the nominal antigen. The authors rationalized their finding by arguing that efficient T-cell activation requires an optimal dwell-time of interaction between TCR and the pMHC. Similarly, Hombrink et al. [57] identified non-responsive human pMHCI tet<sup>+</sup> CD8 T-cell clones isolated from naïve repertoires. Here, the nonreactivity of the pMHCI tet<sup>+</sup> T-cell clones correlated with fast TCR-ligand  $k_{off}$ -rates. In another study using CD8 T-cell clones that bind to pMHCI tet but are refractory to activation by pMHCI ligands, Sibener et al. [58] identified catch bond formation within the TCR-pMHC interface as an essential mechanism for coupling TCR binding to downstream signaling. In the murine influenza virus model, Gras et al. [59] explained the lack of TCR signaling in TRBV17<sup>+</sup> np366-tet<sup>+</sup> CD8 T cells by reversed TCR-pMHC docking modes. Further work is required to determine, if any, of these mechanism(s) explains the impaired responsiveness of gp33-tet<sup>+</sup> T cells in GP<sup>+</sup> mice.

In conclusion, we identified self-pMHCI-tet<sup>+</sup> T cells in mice with robust thymic self-antigen expression. Their ignorance to self-antigen and their TCR signaling behavior to antigen stimu-

lation indicated that they exhibited very low antigen sensitivity. Thus, in the naïve repertoire, self-pMHCI tet staining identifies CD8 T cells that are not self-reactive.

## Materials and methods

### Mice and infections

C57BL/6 (B6) mice were obtained from Janvier (Le Genest-St-Isle, France) or were maintained at the Max Planck Institute of Immunobiology and Epigenetics. P14  $\alpha\beta$ TCR (line 318) [60], P14  $\beta$ TCR (line 128) [31], MHCI.GP (GP<sub>WE</sub>-tg) [38], NP<sub>Arm</sub> [38], and Nur77<sup>GFP</sup>-reporter mice [29] have been described previously. CAG.GP mice were generated by mating Stop-GP<sup>lox</sup> [20] with CMV-Cre mice [61]. Stop-GP<sup>lox</sup> mice contain a *loxP*-flanked STOP cassette followed by LCMV GP, IRES, and yellow fluorescent protein (YFP) sequences in the ROSA26 locus. Offspring of Stop-GP<sup>lox</sup> x CMV-Cre mating with the deleted STOP cassette were identified and mated with B6 mice to remove the CMV-Cre transgene. Afterward, offspring of this mating with deleted STOP cassette and lack of CMV-Cre transgene were further backcrossed to B6 mice to establish the CAG.GP line. Foxn1.GP mice were generated by mating Stop-GP<sup>lox</sup> with Foxn1-Cre mice [62], and offspring were typed for the Cre-transgene. Mice were used for analysis at 7–26 weeks of age. Mice were infected with LCMV Armstrong strain ( $2 \times 10^5$  pfu, intraperitoneally (i.p.)), and all mice were housed under specific pathogen-free conditions. All animal experiments were performed in accordance with the relevant guidelines and regulations approved by the Regierungspräsidium Freiburg, Germany (licenses 35–9185.81; G-15/15, G-20/56, G-22/010).

### PCR typing of mouse lines

All mouse lines used here were kept on a B6 background. They were typed by PCR using the following primers: P14  $\alpha\beta$ TCR and P14  $\beta$ TCR: 5'-GTGCAAAACACATGGAGGCT and 5'-GCGGAAGTG GTTTCGAGGAT; MHCI.GP: 5'-CGACGGCAAGACCACCTGGTGC and 5'-GTTACGGTGGTCTTGAACACGTGC; Nur77/GFP-reporter: 5'-CGGGTCAGAAAG AATGGTGT and 5'-CAGTTTCAGTCCC CATCCTC; CAG.GP: 5'-GGCGCCGGCAGGAAG GAAAT and 5'-CC GTACATGCCACAGGACCTACC; Foxn1.GP: 5'-TGCATGATCTCCG GTATTGA and 5'-CGTACTGACGGTGGGAGAAT. PCR conditions: 95°C 3 min; 35 cycles of 95°C 15 s, 60°C 15 s, 72°C 15 s; and final extension 72°C 1 min using KAPA Mouse Genotyping Kit (KAPABIOSYSTEMS).

### pMHC tetramer-based enrichment and flow cytometry

Single-cell suspension from one spleen or one thymus was stained with PE-labeled pMHCI-tet (5  $\mu$ g) in 500  $\mu$ L IMDM cell culture media containing 10% FCS, anti-CD8 $\alpha$  (clone 53.6.72;

10  $\mu\text{g}/\text{mL}$ ), and anti-CD16/32 mAb (clone 2.4G2, 10  $\mu\text{g}/\text{mL}$ ) at room temperature for 1 h. Cells were then washed once with 15 mL of MACS buffer (PBS, 2 mM EDTA, 0.5% FCS), resuspended in 450  $\mu\text{L}$  MACS buffer, and labeled with 50  $\mu\text{L}$  of anti-PE microbeads (Miltenyi) for 30 min at 4°C. After one wash with 15 mL MACS buffer, cells were resuspended in 3 mL MACS buffer and passed over a magnetized LS column (Miltenyi). The column was washed three times with 3 mL MACS buffer and then removed from the magnet and eluted with 5 mL MACS buffer using a plunger. After centrifugation, cells were resuspended in 250  $\mu\text{L}$  FACS buffer (PBS, 2% FCS, 0.2%  $\text{NaN}_3$ ). Enriched thymocytes were stained with anti-CD4-BV650 (RM4-5), anti-CD8 $\beta$ -APC (H35-17.2), and anti-CD44-BV785 (IM7) mAb for 30 min at 4°. Enriched spleen cells were stained with anti-CD8 $\beta$ -APC (H35-17.2), anti-CD44-BV785 (IM7), anti-B220-PerCP (RA3-6B2), and anti-CD11b-PerCP (M1/70). After washing, entire stained samples were collected on an LSRFortessa flow cytometer (BD Biosciences) and analyzed by FlowJo software 887 (Tree Star). mAbs were obtained from eBioscience or BioLegend. PE-labeled H-2D<sup>b</sup> tet complexed with gp33 (KAVYNEFATM), np396 (FQPQNGQFI), M45 (HGIRNASFI), and PE-labeled H-2K<sup>b</sup> tet complexed B8R (TSYK-FESV) peptides were generated in house. Flow cytometric analysis was performed in accordance with the guidelines for the use of flow cytometry and cell sorting in immunological studies [63]; gating strategies are shown in Supporting Information Fig. 13.

### Adoptive cell transfers

B6.Thy1.1 host mice were pretreated by i.p. injection of 500  $\mu\text{g}$  anti-Thy1.1 mAb (clone 19E12, BioXcel) 1 day before the i.p. injection of  $5 \times 10^7$  total spleen cells from Foxn1.GP<sup>-</sup> or Foxn1.GP<sup>+</sup> mice (both Thy1.2<sup>+</sup>). Two days after cell transfer mice were infected with an LCMV Armstrong strain ( $2 \times 10^5$  pfu, i.p.), and spleen cells were analyzed 8-day pi by flow cytometry using anti-CD8 $\beta$ -APC (H35-17.2), anti-Thy1.1-FITC (HIS51), and anti-Thy1.2-BV650 (30-H12) mAb together with PE-labeled gp33/D<sup>b</sup> tet.

### Immunization and gp33 peptide treatments

Mice were immunized (i.p.) with the indicated amount of gp33 peptide (KAVYNEFATM, Neosystem SA, Strasbourg) together with 50  $\mu\text{g}$  of anti-CD40 mAb (FGK45.5, ichorbio, UK) and 50  $\mu\text{g}$  Poly (I:C) (Miltenyi). After 8 days, spleen cells were analyzed by flow cytometry. For short-term experiments with Nur77/GFP-reporter, mice were injected (i.p.) with the indicated amount of gp33 peptide in PBS and analyzed 6 h later.

### Analysis of thymic LCMV GP expression

LCMV GP expression in thymi of MHC1.GP mice was determined by immunohistology using frozen tissue sections and a rabbit-anti-

LCMV serum as described previously [64]. LCMV GP expression in thymi of CAG.GP and Foxn1.GP mice were determined by flow cytometry using YFP as a co-expressed marker. cTEC and mTEC were isolated as described elsewhere [65] and stained using anti-CD45-PECy7 (30-F11), anti-CD326/EpCAM-APC (G8.8), anti-CD249/BP-1/Ly51-PE (6C3) mAb and biotinylated UEA1-lectin. Thymic DCs were isolated by digestion with collagenase D (0.7 mg/mL) for 1 h at 37°C in a cell culture medium containing 5% FCS followed by purification using anti-CD11c microbeads (Miltenyi). Afterward, cells were stained with anti-CD205-PerCPy5.5 (NLDC-145) and anti-CD4-BV650 (RM4-5) mAb.

### Statistical analysis

To determine *p* values, GraphPad Prism software was used.

**Acknowledgements:** We thank Oliver Schweier for the generation of MHC-monomers and technical assistance in the initial phase of this study. The work was supported by the Max-Planck-Gesellschaft.

Open access funding enabled and organized by Projekt DEAL.

**Conflict of interest:** DDP is a founder, consultant and shareholder of Hookipa Pharma Inc. commercializing arenavirus-based vector technology, and he is listed as an inventor on corresponding patents. The other authors declare no competing interests.

**Author contributions:** Hanspeter Pircher designed research, performed research, analyzed data, and wrote the paper. Daniel D. Pinschewer contributed new reagents/analytic tools and edited the manuscript. Thomas Boehm analyzed data and edited the manuscript.

**Ethics approval statement for animal studies:** The animal experiments were approved by the Regierungspräsidium Freiburg (AZ 35-9185.81/G-15/15; G-19/175; G-22/010) and performed in accordance with the German animal protection law and the directive 2010/63/EU of the European Parliament.

**Data availability statement:** The data that support the findings of this study are available in the manuscript and supplementary material of this article.

**Peer review:** The peer review history for this article is available at <https://publons.com/publon/10.1002/eji.202350402>.

### References

- Altman, J. D., Moss, P. A., Goulder, P. J., Barouch, D. H., McHeyzer-Williams, M. G., Bell, J. I., McMichael, A. J., et al., Phenotypic analysis of antigen-specific T lymphocytes. *Science* 1996. 274: 94–96.

- 2 Altman, J. D. and Davis, M. M., MHC-peptide tetramers to visualize antigen-specific T cells. *Curr. Protoc. Immunol.* 2016. **115**: 171311–171344.
- 3 Davis, M. M., Altman, J. D. and Newell, E. W., Interrogating the repertoire: broadening the scope of peptide-MHC multimer analysis. *Nat. Rev. Immunol.* 2011. **11**: 551–558.
- 4 Dolton, G., Tungatt, K., Lloyd, A., Bianchi, V., Theaker, S. M., Trimby, A., Holland, C. J., et al., More tricks with tetramers: a practical guide to staining T cells with peptide-MHC multimers. *Immunology* 2015. **146**: 11–22.
- 5 Moon, J. J., Chu, H. H., Pepper, M., McSorley, S. J., Jameson, S. C., Kedl, R. M. and Jenkins, M. K., Naive CD4(+) T cell frequency varies for different epitopes and predicts repertoire diversity and response magnitude. *Immunity* 2007. **27**: 203–213.
- 6 Obar, J. J., Khanna, K. M. and Lefrancois, L., Endogenous naive CD8+ T cell precursor frequency regulates primary and memory responses to infection. *Immunity* 2008. **28**: 859–869.
- 7 Su, L. F., Kidd, B. A., Han, A., Kotzin, J. J. and Davis, M. M., Virus-specific CD4(+) memory-phenotype T cells are abundant in unexposed adults. *Immunity* 2013. **38**: 373–383.
- 8 Nelson, R. W., Beisang, D., Tubo, N. J., Dileepan, T., Wiesner, D. L., Nielsen, K., Wuthrich, M., et al., T cell receptor cross-reactivity between similar foreign and self peptides influences naive cell population size and autoimmunity. *Immunity* 2015. **42**: 95–107.
- 9 Hassler, T., Urmann, E., Teschner, S., Federle, C., Dileepan, T., Schober, K., Jenkins, M. K., et al., Inventories of naive and tolerant mouse CD4 T cell repertoires reveal a hierarchy of deleted and diverted T cell receptors. *Proc. Natl. Acad. Sci. USA* 2019. **116**: 18537–18543.
- 10 Legoux, F. P., Lim, J. B., Cauley, A. W., Dikiy, S., Ertelt, J., Mariani, T. J., Sparwasser, T., et al., CD4+ T cell tolerance to tissue-restricted self antigens is mediated by antigen-specific regulatory T cells rather than deletion. *Immunity* 2015. **43**: 896–908.
- 11 Malhotra, D., Linehan, J. L., Dileepan, T., Lee, Y. J., Purtha, W. E., Lu, J. V., Nelson, R. W., et al., Tolerance is established in polyclonal CD4(+) T cells by distinct mechanisms, according to self-peptide expression patterns. *Nat. Immunol.* 2016. **17**: 187–195.
- 12 Moon, J. J., Dash, P., Oguin, T. H., 3rd, McClaren, J. L., Chu, H. H., Thomas, P. G. and Jenkins, M. K., Quantitative impact of thymic selection on Foxp3+ and Foxp3- subsets of self-peptide/MHC class II-specific CD4+ T cells. *Proc. Natl. Acad. Sci. USA* 2011. **108**: 14602–14607.
- 13 Hogquist, K. A., Baldwin, T. A. and Jameson, S. C., Central tolerance: learning self-control in the thymus. *Nat. Rev. Immunol.* 2005. **5**: 772–782.
- 14 Jensen, K. D., Su, X., Shin, S., Li, L., Youssef, S., Yamasaki, S., Steinman, L., et al., Thymic selection determines gammadelta T cell effector fate: antigen-naive cells make interleukin-17 and antigen-experienced cells make interferon gamma. *Immunity* 2008. **29**: 90–100.
- 15 Yu, W., Jiang, N., Ebert, P. J., Kidd, B. A., Muller, S., Lund, P. J., Juang, J., et al., Clonal deletion prunes but does not eliminate self-specific alpha-beta CD8(+) T lymphocytes. *Immunity* 2015. **42**: 929–941.
- 16 Pircher, H., Rohrer, U. H., Moskophidis, D., Zinkernagel, R. M. and Hengartner, H., Lower receptor avidity required for thymic clonal deletion than for effector T-cell function. *Nature* 1991. **351**: 482–485.
- 17 Vasquez, N. J., Kaye, J. and Hedrick, S. M., In vivo and in vitro clonal deletion of double-positive thymocytes. *J. Exp. Med.* 1992. **175**: 1307–1316.
- 18 Davey, G. M., Schober, S. L., Endrizzi, B. T., Dutcher, A. K., Jameson, S. C. and Hogquist, K. A., Preselection thymocytes are more sensitive to T cell receptor stimulation than mature T cells. *J. Exp. Med.* 1998. **188**: 1867–1874.
- 19 Sant'Angelo, D. B. and Janeway, C. A., Jr., Negative selection of thymocytes expressing the D10 TCR. *Proc. Natl. Acad. Sci. USA* 2002. **99**: 6931–6936.
- 20 Page, N., Klimek, B., De Roo, M., Steinbach, K., Soldati, H., Lemeille, S., Wagner, I., et al., Expression of the DNA-binding factor TOX promotes the encephalitogenic potential of microbe-induced autoreactive CD8(+) T cells. *Immunity* 2018. **48**: 937–950.e938.
- 21 Kisielow, P., Bluthmann, H., Staerz, U. D., Steinmetz, M. and von Boehmer, H., Tolerance in T-cell-receptor transgenic mice involves deletion of non-mature CD4+8+ thymocytes. *Nature* 1988. **333**: 742–746.
- 22 Knobloch, M., Schonrich, G., Schenkel, J., Malissen, M., Malissen, B., Schmitt-Verhulst, A. M., Hammerling, G. J., et al., T cell activation and thymic tolerance induction require different adhesion intensities of the CD8 co-receptor. *Int. Immunol.* 1992. **4**: 1169–1174.
- 23 Teh, H. S., Kishi, H., Scott, B. and Von Boehmer, H., Deletion of autospesific T cells in T cell receptor (TCR) transgenic mice spares cells with normal TCR levels and low levels of CD8 molecules. *J. Exp. Med.* 1989. **169**: 795–806.
- 24 von Boehmer, H., Kirberg, J. and Rocha, B., An unusual lineage of alpha/beta T cells that contains autoreactive cells. *J. Exp. Med.* 1991. **174**: 1001–1008.
- 25 Baldwin, T. A., Sandau, M. M., Jameson, S. C. and Hogquist, K. A., The timing of TCR alpha expression critically influences T cell development and selection. *J. Exp. Med.* 2005. **202**: 111–121.
- 26 Bruno, L., Fehling, H. J. and von Boehmer, H., The alpha beta T cell receptor can replace the gamma delta receptor in the development of gamma delta lineage cells. *Immunity* 1996. **5**: 343–352.
- 27 Egawa, T., Kreslavsky, T., Littman, D. R. and von Boehmer, H., Lineage diversion of T cell receptor transgenic thymocytes revealed by lineage fate mapping. *PLoS One* 2008. **3**: e1512.
- 28 Terrence, K., Pavlovich, C. P., Matechak, E. O. and Fowlkes, B. J., Premature expression of T cell receptor (TCR)alphabeta suppresses TCRgammadelta gene rearrangement but permits development of gammadelta lineage T cells. *J. Exp. Med.* 2000. **192**: 537–548.
- 29 Moran, A. E., Holzapfel, K. L., Xing, Y., Cunningham, N. R., Maltzman, J. S., Punt, J. and Hogquist, K. A., T cell receptor signal strength in Treg and iNKT cell development demonstrated by a novel fluorescent reporter mouse. *J. Exp. Med.* 2011. **208**: 1279–1289.
- 30 Hogquist, K. A., Jameson, S. C., Heath, W. R., Howard, J. L., Bevan, M. J. and Carbone, F. R., T cell receptor antagonist peptides induce positive selection. *Cell* 1994. **76**: 17–27.
- 31 Pircher, H., Mak, T. W., Lang, R., Ballhausen, W., Ruedi, E., Hengartner, H., Zinkernagel, R. M., et al., T cell tolerance to Mlsa encoded antigens in T cell receptor V beta 8.1 chain transgenic mice. *EMBO J.* 1989. **8**: 719–727.
- 32 Brandle, D., Burki, K., Wallace, V. A., Rohrer, U. H., Mak, T. W., Malissen, B., Hengartner, H., et al., Involvement of both T cell receptor V alpha and V beta variable region domains and alpha chain junctional region in viral antigen recognition. *Eur. J. Immunol.* 1991. **21**: 2195–2202.
- 33 Bouneaud, C., Kourilsky, P. and Bousso, P., Impact of negative selection on the T cell repertoire reactive to a self-peptide: a large fraction of T cell clones escapes clonal deletion. *Immunity* 2000. **13**: 829–840.
- 34 Busch, D. H. and Pamer, E. G., T cell affinity maturation by selective expansion during infection. *J. Exp. Med.* 1999. **189**: 701–710.
- 35 Crawford, F., Kozono, H., White, J., Marrack, P. and Kappler, J., Detection of antigen-specific T cells with multivalent soluble class II MHC covalent peptide complexes. *Immunity* 1998. **8**: 675–682.
- 36 Savage, P. A., Boniface, J. J. and Davis, M. M., A kinetic basis for T cell receptor repertoire selection during an immune response. *Immunity* 1999. **10**: 485–492.
- 37 Zehn, D. and Bevan, M. J., T cells with low avidity for a tissue-restricted antigen routinely evade central and peripheral tolerance and cause autoimmunity. *Immunity* 2006. **25**: 261–270.

- 38 Wooten, C., Straub, T., Schweier, O., Aichele, U., Duker, K., Boehm, T. and Pircher, H., Immunological tolerance to LCMV antigens differently affects control of acute and chronic virus infection in mice. *Eur. J. Immunol.* 2018. 48: 120–127.
- 39 Cho, H. I. and Celis, E., Optimized peptide vaccines eliciting extensive CD8 T-cell responses with therapeutic antitumor effects. *Cancer Res.* 2009. 69: 9012–9019.
- 40 Grossman, Z. and Paul, W. E., Dynamic tuning of lymphocytes: physiological basis, mechanisms, and function. *Annu. Rev. Immunol.* 2015. 33: 677–713.
- 41 Truckenbrod, E. N., Burrack, K. S., Knutson, T. P., Borges da Silva, H., Block, K. E., O'Flanagan, S. D., Stagliano, K. R., et al., CD8(+) T cell self-tolerance permits responsiveness but limits tissue damage. *Elife* 2021. 10: e65615.
- 42 Trager, U., Sierro, S., Djordjevic, G., Bouzo, B., Khandwala, S., Meloni, A., Mortensen, M., et al., The immune response to melanoma is limited by thymic selection of self-antigens. *PLoS One* 2012. 7: e35005.
- 43 Culina, S., Lalanne, A. I., Afonso, G., Cerosaletti, K., Pinto, S., Sebastiani, G., Kuranda, K., et al., Islet-reactive CD8(+) T cell frequencies in the pancreas, but not in blood, distinguish type 1 diabetic patients from healthy donors. *Sci. Immunol.* 2018. 3: eaao4013.
- 44 Maeda, Y., Nishikawa, H., Sugiyama, D., Ha, D., Hamaguchi, M., Saito, T., Nishioka, M., et al., Detection of self-reactive CD8(+) T cells with an anergic phenotype in healthy individuals. *Science* 2014. 346: 1536–1540.
- 45 Pittet, M. J., Valmori, D., Dunbar, P. R., Speiser, D. E., Lienard, D., Lejeune, F., Fleischhauer, K., et al., High frequencies of naive Melan-A/MART-1-specific CD8(+) T cells in a large proportion of human histocompatibility leukocyte antigen (HLA)-A2 individuals. *J. Exp. Med.* 1999. 190: 705–715.
- 46 Velthuis, J. H., Unger, W. W., Abreu, J. R., Duinkerken, G., Franken, K., Peakman, M., Bakker, A. H., et al., Simultaneous detection of circulating autoreactive CD8+ T-cells specific for different islet cell-associated epitopes using combinatorial MHC multimers. *Diabetes* 2010. 59: 1721–1730.
- 47 Ohashi, P. S., Oehen, S., Buerki, K., Pircher, H., Ohashi, C. T., Odermatt, B., Malissen, B., et al., Ablation of “tolerance” and induction of diabetes by virus infection in viral antigen transgenic mice. *Cell* 1991. 65: 305–317.
- 48 Oldstone, M. B., Nerenberg, M., Southern, P., Price, J. and Lewicki, H., Virus infection triggers insulin-dependent diabetes mellitus in a transgenic model: role of anti-self (virus) immune response. *Cell* 1991. 65: 319–331.
- 49 Murali-Krishna, K., Altman, J. D., Suresh, M., Sourdive, D. J., Zajac, A. J., Miller, J. D., Slansky, J., et al., Counting antigen-specific CD8 T cells: a reevaluation of bystander activation during viral infection. *Immunity* 1998. 8: 177–187.
- 50 Sabatino, J. J., Jr., Huang, J., Zhu, C. and Evavold, B. D., High prevalence of low affinity peptide-MHC II tetramer-negative effectors during polyclonal CD4+ T cell responses. *J. Exp. Med.* 2011. 208: 81–90.
- 51 Martinez, R. J., Andargachew, R., Martinez, H. A. and Evavold, B. D., Low-affinity CD4+ T cells are major responders in the primary immune response. *Nat. Commun.* 2016. 7: 13848.
- 52 Daniels, M. A. and Jameson, S. C., Critical role for CD8 in T cell receptor binding and activation by peptide/major histocompatibility complex multimers. *J. Exp. Med.* 2000. 191: 335–346.
- 53 Zhang, Z., Legoux, F. P., Vaughan, S. W. and Moon, J. J., Opposing peripheral fates of tissue-restricted self antigen-specific conventional and regulatory CD4(+) T cells. *Eur. J. Immunol.* 2020. 50: 63–72.
- 54 Coles, R. M., Jones, C. M., Brooks, A. G., Cameron, P. U., Heath, W. R. and Carbone, F. R., Virus infection expands a biased subset of T cells that bind tetrameric class I peptide complexes. *Eur. J. Immunol.* 2003. 33: 1557–1567.
- 55 Malherbe, L., Hausl, C., Teyton, L. and McHeyzer-Williams, M. G., Clonal selection of helper T cells is determined by an affinity threshold with no further skewing of TCR binding properties. *Immunity* 2004. 21: 669–679.
- 56 Kalergis, A. M., Boucheron, N., Doucey, M. A., Palmieri, E., Goyarts, E. C., Vegh, Z., Luescher, I. F., et al., Efficient T cell activation requires an optimal dwell-time of interaction between the TCR and the pMHC complex. *Nat. Immunol.* 2001. 2: 229–234.
- 57 Hombrink, P., Raz, Y., Kester, M. G., de Boer, R., Weissbrich, B., von dem Borne, P. A., Busch, D. H., et al., Mixed functional characteristics correlating with TCR-ligand koff-rate of MHC-tetramer reactive T cells within the naive T-cell repertoire. *Eur. J. Immunol.* 2013. 43: 3038–3050.
- 58 Sibener, L. V., Fernandes, R. A., Kolawole, E. M., Carbone, C. B., Liu, F., McAfee, D., Birnbaum, M. E., et al., Isolation of a structural mechanism for uncoupling T cell receptor signaling from peptide-MHC binding. *Cell* 2018. 174: 672–687 e627.
- 59 Gras, S., Chadderton, J., Del Campo, C. M., Farenc, C., Wiede, F., Josephs, T. M., Sng, X. Y. X., et al., Reversed T cell receptor docking on a major histocompatibility class I complex limits involvement in the immune response. *Immunity* 2016. 45: 749–760.
- 60 Pircher, H., Burki, K., Lang, R., Hengartner, H. and Zinkernagel, R. M., Tolerance induction in double specific T-cell receptor transgenic mice varies with antigen. *Nature* 1989. 342: 559–561.
- 61 Schwenk, F., Baron, U. and Rajewsky, K., A cre-transgenic mouse strain for the ubiquitous deletion of loxP-flanked gene segments including deletion in germ cells. *Nucleic. Acids. Res.* 1995. 23: 5080–5081.
- 62 Soza-Ried, C., Bleul, C. C., Schorpp, M. and Boehm, T., Maintenance of thymic epithelial phenotype requires extrinsic signals in mouse and zebrafish. *J. Immunol.* 2008. 181: 5272–5277.
- 63 Cossarizza, A., Chang, H. D., Radbruch, A., Abignani, S., Addo, R., Akdis, M., Andra, I., et al., Guidelines for the use of flow cytometry and cell sorting in immunological studies (third edition). *Eur. J. Immunol.* 2021. 51: 2708–3145.
- 64 Straub, T. and Pircher, H., Enhancing immunity prevents virus-induced T-cell-mediated immunopathology in B cell-deficient mice. *Eur. J. Immunol.* 2019. 49: 782–789.
- 65 Nagakubo, D., Krauth, B. and Boehm, T., Genetic and non-genetic determinants of thymic epithelial cell number and function. *Sci. Rep.* 2017. 7: 10314.

**Abbreviations:** **i.p.:** intraperitoneally · **IRES:** internal ribosomal entry site · **LCMV:** lymphocytic choriomeningitis virus · **NP:** nucleoprotein · **pMHC:** peptide-MHC · **SP:** single positive · **tet:** tetramers · **tg:** transgenic · **Trp2:** tyrosinase-related protein 2 · **YFP:** yellow fluorescent protein

**Full correspondence:** Prof. Hanspeter Pircher, Department of Developmental Immunology, Max Planck Institute of Immunobiology and Epigenetics, 79108 Freiburg im Breisgau, Germany  
e-mail: pircher@ie-freiburg.mpg.de

Received: 23/1/2023  
Revised: 19/4/2023  
Accepted: 9/5/2023  
Accepted article online: 14/5/2023